Simulation of Electromagnetic-Acoustic Coupling in Piezoelectric Devices Using FEM Software beyond Quasi-static Approximation

Xiaotian Xu, *Member, IEEE,*

***Abstract*—A method of simulating electromagnetic-acoustic coupling on piezoelectric devices is introduced in this paper. This method is based on weak form and can be applied in any finite-element method (FEM) software. As no quasi-static approximation is imposed, magnetic fields can also be simulated. The application of this method in COMSOL Multiphysics is demonstrated as an example. The accuracy and ability of the simulation are verified by simulating Rayleigh mode on a piezoelectric waveguide and torsional mode on a cylinder resonator.**

***Index Terms*—surface acoustic wave, piezoelectricity, beyond quasi-static approximation, COMSOL, Rayleigh mode, torsional mode, waveguide, antenna, weak form, quantum computing**

I. Introduction

PIEZOELECTRIC material is a kind of anisotropic material that enables transformation between acoustic energy and electromagnetic energy. Hybrid vibration (both electromagnetic and acoustic) can be induced using electrodes attached to the piezoelectric material. An electromagnetic-acoustic (EMA) coupling appears in this vibration.

One example of EMA coupling is surface acoustic waves (SAWs) on a piezoelectric waveguide. SAWs are hybrid waves bonded at the surface of a waveguide. Both acoustic and electromagnetic parts propagate along the extensional direction with the same frequency and wavenumber. These two parts are identical in the transverse direction. Piezoelectric waveguides have various applications, such as delay lines, filters and resonators. It can also be used in quantum systems, for example, as a media in the coupling between phonons and artificial atoms [1].

Another example of EMA coupling is a piezoelectric antenna. Piezoelectric antennas have advantages over conventional antennas. The dimension of a conventional antenna needs to be similar to the wavelength of the resonant electromagnetic wave, which is at least 1 mm at radio frequency. This requirement hinders a conventional antenna from being applied to small devices like mobile phones, especially in the low-frequency commutation domain. Relatively, the size of a piezoelectric antenna is approximately 10^{-5} times smaller because this size only needs to have the same order as acoustic waves' wavelength.

This paper was produced by the IEEE Publication Technology Group. They are in Piscataway, NJ.

Manuscript received April 19, 2021; revised August 16, 2021.

Owing to the anisotropy of the media, the simulation of the EMA coupling on piezoelectric devices is usually complex. A quasi-static approximation is thus often applied to reduce this complexity. Under this approximation, the magnetic field is neglected, and the negative divergence of electric potential represents the electric field strength. In most circumstances, this approximation works well because the magnetic field is generally far less robust than the electric field [2]. However, some researches focus more on the magnetic field, like the analysis of antennas [3], where quasi-static approximation should be avoided.

There are certain analytical methods that can precisely simulate the EMA coupling without using quasi-static approximation. Examples include the superposition of partial waves method [2], transverse resonance method [4], Kirchhoff plate theory method [5], [6]. These methods are limited to specific geometries and lattice structures, making them less universal. However, universal FEM simulating software, like COMSOL Multiphysics, always uses quasi-static approximation. Our method is applicable in any FEM simulating software, where weak forms describe the whole coupling system, including the magnetic fields. COMSOL is used as an example to demonstrate the configuration and arrive at results, some of which are subsequently analysed. The results corresponding to the Rayleigh mode on piezoelectric waveguides is compared with experimental results and analytical results, to validate the accuracy. The results corresponding to the torsional mode on a cylinder piezoelectric antenna indicate the ability to simulate complicated devices. Definition of variables, codes and more details in building a simulation are mentioned in the Supplementary Material.

II. Methodology

A. Weak Forms

The total energy density U at an arbitrary point is represented using 8 variables: velocity $\underline{v}$, momentum $\underline{p}$, strain $\underline{\underline{S}}$, stress $\underline{\underline{T}}$, electric field strength $\underline{E}$, electric displacement $\underline{D}$, magnetic field strength $\underline{H}$ and magnetic flux density $\underline{B}$ [2].

$$2U = \underline{v} \cdot \underline{p} + \underline{\underline{S}} : \underline{\underline{T}} + \underline{E} \cdot \underline{D} + \underline{H} \cdot \underline{B} \tag{1}$$

The weak form is written as an integration of the negative total energy density throughout the space, where one of the

0000–0000/00$00.00 © 2021 IEEE

two variables in each term is replaced with a test function (denoted by "˜"):

$$\int_V -\left(\tilde{\underline{v}}\cdot\underline{p}+\tilde{\underline{\underline{S}}}:\underline{\underline{T}}+\tilde{\underline{E}}\cdot\underline{D}+\tilde{\underline{H}}\cdot\underline{B}\right)=0 \tag{2}$$

In a piezoelectric material, the coupling between acoustic fields and electromagnetic fields is described as constitutive relations

$$\underline{\underline{T}} = \underline{\underline{\underline{c}}}^{E}:\underline{\underline{S}}-\underline{\underline{e}}^{T}\cdot\underline{E} \tag{3a}$$

$$\underline{D} = \underline{\underline{e}}:\underline{\underline{S}}+\underline{\underline{\epsilon}}^{S}\cdot\underline{E} \tag{3b}$$

where $\underline{\underline{\underline{c}}}^{E}$ is the stiffness tensor at zero or constant electric field strength, $\underline{\underline{e}}$ and $\underline{\underline{e}}^{T}$ are piezoelectric coupling tensor and its transpose, $\underline{\underline{\epsilon}}^{S}$ is the permittivity matrix at zero or constant strain. The number of underlines ("_") denotes the rank of this tensor.

Magnetisation relation and Maxwell's equation are used to describe the relation between electric fields and magnetic fields.

$$\underline{H}=\frac{\underline{B}}{\mu_0} \tag{4a}$$

$$\nabla\times\vec{E}=-\frac{\partial\vec{B}}{\partial t} \tag{4b}$$

(3a), (3b), (4a) and (4b) enable (2) to be represented by only two variables $\underline{u}$ and $\underline{E}$. In COMSOL, these two variables are named *Dependent Variables* which are defined when establishing a new model. The components of (2) then serves as the input into *Weak Form PDE* and *Weak Contribution* nodes in different physics interfaces. The detailed processes are introduced in the Supplementary Material.

B. M-field Method

As mentioned in Section A, the components of electric field strength $\{E_x, E_y, E_z\}$ are usually chosen as dependent variables in an electromagnetic field. The subsequent derivation of the magnetic field strength inevitably includes a division of angular frequency ω. However, this division is forbidden in COMSOL (error information: "Division by zero"). Except using the iteration method, this problem can also be solved by setting M-field components $\{M_x, M_y, M_z\}$ as dependent variables. These variables are defined as

$$M_x=\frac{E_x}{\omega},\ M_y=\frac{E_y}{\omega},\ M_z=\frac{E_z}{\omega} \tag{5}$$

Then, the magnetic field strength can be directly derived from the variables $\{M_x, M_y, M_z\}$ without ω. Nodes in the electromagnetic field, such as constraints and boundary conditions, are also based on M-field.

C. Boundary Conditions

In COMSOL, each boundary requires at least one boundary condition. A proper boundary condition can increase the accuracy and reduce the time of calculation. This section introduces all boundary conditions used in our method, which are based on nodes provided in *weak form PDE* interface.

1) Fixed Boundary Condition: On some boundaries which waves cannot (or barely) reach, the fixed boundary conditions is a efficient choice. This boundary condition is realised using *Dirichlet Boundary Condition* node, where all three input boxes are filled with zeros.

2) Periodic Boundary Condition: When analysing some models like infinitely long waveguides, the periodic boundary condition is inevitable. This boundary condition truncates the propagating distance to some integral multiples of the wavelength. It should be applied on the boundaries normal to the propagating direction. Moreover, the periodic boundary condition can be applied when waves are identical in one direction. It should be applied on boundaries normal to this direction.

Periodic Condition node is provided by *weak form PDE* interface.

3) Free Boundary Condition and Continuity Boundary Condition: On the interface between a piezoelectric material and the air, the propagation of an acoustic wave stops but the propagation of an electromagnetic wave does not. Thus, the free boundary condition should be applied here for acoustic waves and the continuous boundary condition for the electromagnetic field.

For electromagnetic fields on both sides, the tangential part of $\underline{E}$ and $\underline{H}$ and the vertical part of $\underline{D}$ and $\underline{E}$ are the same.

$$(\underline{E_1}-\underline{E_2})\times\hat{n}=0 \tag{6a}$$

$$(\underline{H_1}-\underline{H_2})\times\hat{n}=0 \tag{6b}$$

$$(\underline{D_1}-\underline{D_2})\cdot\hat{n}=0 \tag{6c}$$

$$(\underline{B_1}-\underline{B_2})\cdot\hat{n}=0 \tag{6d}$$

Only one of these conditions is enough for an interface.

The free boundary condition can be realised using the default *Zero Flux* node. The continuity boundary condition can be realised using the *Pointwise Constraint* node, and its configuration can be found in Supplementary Material.

4) Electric-Wall Boundary Condition: In some models, the piezoelectric device is placed in a cavity enclosed by perfectly conductive walls. The Electric-wall boundary condition can accurately represent those walls while avoiding introducing a specific material or a new calculation region. This condition constrains both the tangential part of electric field strength and the normal part of magnetic field strength to be zero.

$$\underline{H}\cdot\hat{n}=0 \tag{7a}$$

$$\underline{E}\times\hat{n}=0 \tag{7b}$$

Only the constraints on electric fields are enough.

These constraints are applied using three *Pointwise Constraint* nodes.

5) Absorbing Boundary Condition: An Absorbing boundary condition (ABC) is applied to truncate the calculation region to a reasonable size. Without the ABC, the radiating electromagnetic wave will reflect the truncating surfaces and disturb wave patterns in the calculation region. The ABC can reduce this reflection. The ABC is in the form of a constraint

and does not need a different region. The explicit form of the first order ABC is [7]:

$$\hat{r} \times \nabla \times \underline{E} = jk\underline{E}_t - (s-1)\nabla_t E_r \tag{8}$$

where s is a factor and $s = 0.5$ gives the minimum reflection [7]. In COMSOL, (8) is separated into three direction and written into three *Pointwise Constrain* nodes.

D. Magnetic Coupling Coefficient

The strength of EMA coupling is one of judgement on the performance of a piezoelectric device. This strength can be indicated using a magnetic coupling coefficient, which is defined as

$$\eta = \frac{E_{\text{mag}}^{\text{ext}}}{E_{\text{kin}}^{\text{int}} + E_{\text{ela}}^{\text{int}} + E_{\text{elec}}^{\text{int}} + E_{\text{mag}}^{\text{int}} + E_{\text{elec}}^{\text{ext}} + E_{\text{mag}}^{\text{ext}}} \tag{9}$$

where E_{kin}, E_{ela}, E_{elec} and E_{mag} denote kinetic energy, elastic energy, electric energy and magnetic energy, respectively. The superscripts "int" and "ext" denote internal field (within the piezoelectric substrate) and external field (in the environment). Each energy is calculated using an integration of corresponding energy density throughout its area.

III. Example Applications

A. Rayleigh Mode on a SAW Waveguide

In a SAW waveguide, the transmission part is mainly focused on, instead of IDTs or receivers. Thus this waveguide model can be simplified into two cuboids. One represents the piezoelectric substrate, where the transmission happens. The other represents the surrounding environment. These two cuboids are divided by the surface of the waveguide. Spatial coordinate axes are chosen such that x is along the direction of propagation, y is in the surface and perpendicular to x, while z is outward normal to the surface. When no rotation is applied, the material coordinates match the spatial coordinates.

Rayleigh mode usually has a significant magnetic field, so our verification mainly focuses on this mode. Boundary conditions suitable for this mode are applied. A periodic boundary condition is applied on the propagating direction (surfaces ① & ② and their opposites in Fig.1(1)). The distance between those two surfaces is set as 100 μm, and this distance will become the wavelength of the Rayleigh mode. Another periodic boundary condition is applied in y direction (surfaces ④ & ⑤ and their opposites in Fig.1(1)). Since the Rayleigh mode is identical in this direction, the distance between the two surfaces will not influence the wave behaviour. This distance is set as 10 μm. The fixed constrain is applied in z direction (surface ③ and its opposite in Fig.1(1)). The Rayleigh mode is evanescent in this direction so that 300 μm, which is three times as long as the wavelength, is set as the distance from the surface to the fixed constrain. The electromagnetic continuity boundary condition is applied on surface ⑥, whereas this boundary is set as a free boundary for the acoustic field. For some metallised surfaces, an electric-wall boundary condition needs to be applied on surface ⑥. In this simulation, $z < 0$ (Area **A** in Fig.1(1)) is filled with piezoelectric material and $z > 0$ (Area **B** in Fig.1(1)) is chosen to be air. COMSOL build-in material properties are used.

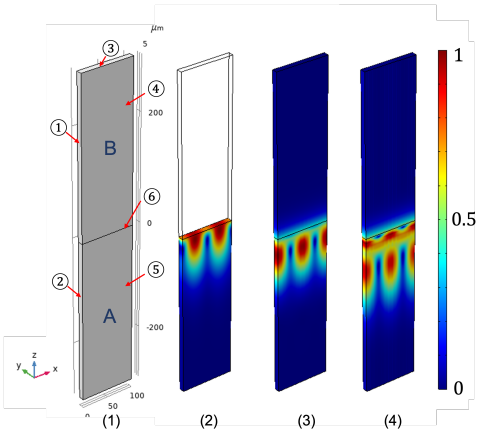

Fig. 1. (1) Geometry of the waveguide model. "A" and "B" symbolise the areas of piezoelectric substrate and air, respectively. The simulation result of unified (2) acoustic wave, (3) electric wave and (4) magnetic wave patterns for the Rayleigh mode on X-prop Z-cut $LiNbO_3$ are shown. Those three waves already significantly decayed before reaching the fixed boundary. Relative to the magnetic field in the substrate, the magnetic field in the environment is much weaker.

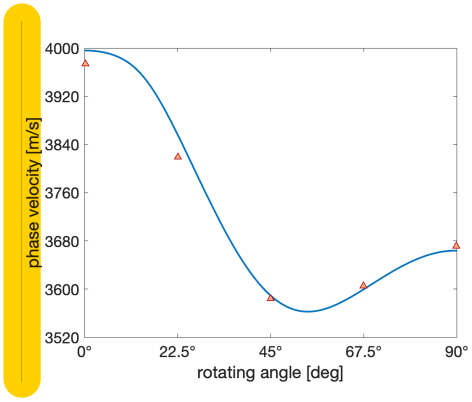

Fig. 2. Comparison of simulated (blue line) and measured [9] (amber triangles) Rayleigh Velocities corresponding to different propagating directions on 128°Y-cut $LiNbO_3$. In the simulation, the propagating direction is initially along X-axis and then rotates anti-clockwise.

The acoustic field, electric field and magnetic field of the Rayleigh mode on X-prop Z-cut $LiNbO_3$ are illustrated in Fig.1 (2), (3) and (4), respectively. Unification is used. Comparison among experimental results, analytical results and our FEM method results of SAW velocities is shown in TABLE I. Velocities of different materials and different modes with different boundaries are included. The analytical results are calculated by the author using the method introduced by Tseng [8]. Please notice the build-in density of CdS and ZnO are different from standard value, so that they are replaced. Furthermore, the slowness surface of 128°Y-cut $LiNbO_3$ is simulated and plotted (Fig. 2). Experimental results [9] are also included for comparison.

B. T_{00} Torsional Mode of a Cylinder Antenna

The torsional mode also has a significant magnetic field. This mode keeps particles on the equatorial plane and the z-axis motionless, and the other particles rotate around the

TABLE I
COMPARISON BETWEEN VELOCITIES OBTAINED FROM METHODS.

Material	Mode	Boundary	Direction	Experimental Result (m/s)	Analytical Result (m/s)	FEM Result (m/s)
CdS	Rayleigh	Free	X-prop Y-cut	1730 [10]	1731.0007	1730.8
ZnO	Rayleigh	Free	X-prop Y-cut	2690 [8]	2697.8171	2697.9
PZT-4	Rayleigh	Free	X-prop Y-cut	2120 [11]	2241.8391	2242.1
PZT-5H	Rayleigh	Free	X-prop Y-cut	-	2038.4889	2038.5
PZT-5A	Rayleigh	Free	X-prop Y-cut	-	1977.6175	1977.8
$LiTaO_3$	Rayleigh	Free	X-prop 36°Y-cut	3124 [12]	-	3112.1999
$LiTaO_3$	Rayleigh	Metallised	X-prop 36°Y-cut	3122 [12]	-	3112.1864
$LiTaO_3$	Leaky	Metallised	X-prop 36°Y-cut	4099 [12]	-	4072.8153

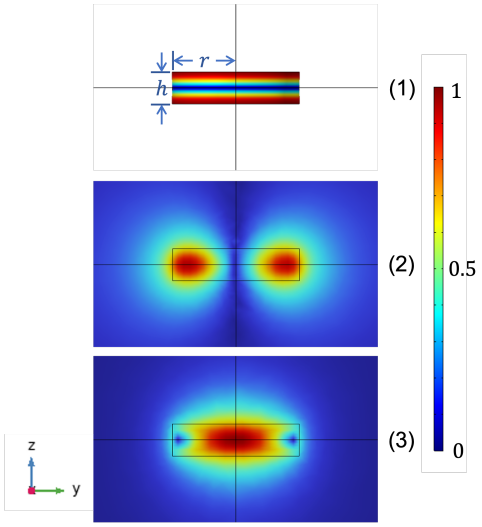

Fig. 3. Unified (1) acoustic field (2) electric field and (3) magnetic field on the YZ section of a PZT-5H cylinder. The height and radius of this cylinder are 5 mm and 10 mm, respectively. The frequency of this mode is 175.12 kHz. Rotation directions on different sides are opposite from each other. The torsion generates a rotational electric field concentrated at the arc-shaped surface of the cylinder. This solenoid-like electric field then induces a magnetic field concentrated at the centre.

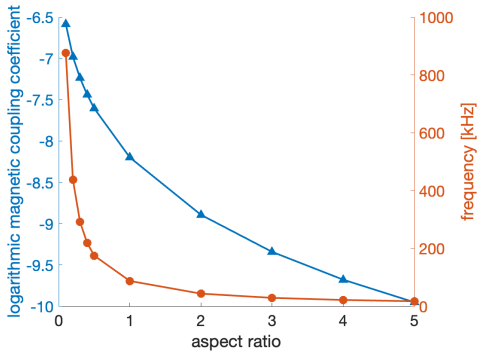

Fig. 4. The relation between aspect ratio and frequency (amber circles) & magnetic coupling coefficients (blue triangles) of T_{00} torsional mode. Amber and blue lines are straight lines connecting them to demonstrate the trend. Simulations were conductd on a PZT-5H cylinder with a 10 mm radius. The radius of the environment sphere is 300 mm. When the aspect decrease (the cylinder looks more like a disk), both frequency and magnetic coupling coefficient will increase. The magnetic coupling coefficient can reach 2.6×10^{-7} when the aspect ratio is 0.1.

z-axis. This rotation becomes more significant if the particle is farther from the origin (shown in Fig.3(1)). In uni-axial materials like PZT-5H, this mode is significant. A cylinder made with other material, like $LiNbO_3$, will show torsional mode only when the aspect ratio (defined as the ratio of height to the radius h/r) is not so small.

A series of simulations were conducted on PZT-5H cylinders. The radii of those cylinders are the same (10 μm), and heights change from 1 mm to 5 mm. These cylinders are placed at the centre of a sphere, representing the surrounding environment. The continuous boundary condition is applied to the cylinder and the sphere interface. Meanwhile, the absorbing boundary condition is applied on the sphere's outer surface. The acoustic field, electric field and magnetic field on the YZ cross-section are shown in Fig.3 as an example. It is found that when the aspect ratio decrease, both the magnetic coupling coefficient and frequency will increase. The relation among those three quantities is shown in Fig. 4.

IV. CONCLUSION

We reported a method for simulation of electromagnetic-acoustic coupling on piezoelectric devices. Our method is beyond quasi-static approximation so that the magnetic field can also be simulated. Two test cases were demonstrated. The Rayleigh-mode waveforms on a waveguide were plotted. The Rayleigh velocities on different materials were compared with experimental results. Furthermore, one of the torsional modes on a cylinder antenna was plotted. The relation between the aspect ratio, resonant frequencies, and magnetic coupling coefficients was studied.

ACKNOWLEDGMENTS

This should be a simple paragraph before the References to thank those individuals and institutions who have supported your work on this article.

REFERENCES

[1] M. V. Gustafsson, T. Aref, A. F. Kockum, M. K. Ekström, G. Johansson, and P. Delsing, "Propagating phonons coupled to an artificial atom," *Science*, vol. 346, no. 6206, pp. 207–211, Oct. 2014. [Online]. Available: https://www.science.org/doi/10.1126/science.1257219

[2] B. A. Auld, *Acoustic Fields and Waves in Solids*. New York ;: Wiley, 1973, publication Title: Acoustic fields and waves in solids.

[3] M. A. Kemp, M. Franzi, A. Haase, E. Jongewaard, M. T. Whittaker, M. Kirkpatrick, and R. Sparr, "A high Q piezoelectric resonator as a portable VLF transmitter," *Nature Communications*, vol. 10, no. 1, 2019.

[4] C. Tseng, "Elastic Surface Waves on Free Surface and Metallized Surface of CdS, ZnO, and PZT-4," *Journal of Applied Physics*, vol. 38, no. 11, pp. 4281–4284, Oct. 1967. [Online]. Available: http://aip.scitation.org/doi/10.1063/1.1709116

[5] J. McKenna, G. D. Boyd, and R. N. Thurston, "Plate Theory Solution for Guided Flexural Acoustic Waves Along the Tip of a Wedge," *IEEE Transactions on Sonics and Ultrasonics*, vol. 21, no. 3, pp. 178–186, 1974.
[6] S. P. Timošenko and S. Woinowsky-Krieger, *Theory of plates and shells*, 2nd ed., ser. Engineering societies monographs. New York: McGraw-Hill, 1987, oCLC: 256657700.
[7] J.-M. Jin, *The Finite Element Method in Electromagnetics*, 2nd ed. New York: Wiley, 2002.
[8] C. Tseng and R. M. White, "Propagation of Piezoelectric and Elastic Surface Waves on the Basal Plane of Hexagonal Piezoelectric Crystals," *Journal of Applied Physics*, vol. 38, no. 11, pp. 4274–4280, 1967.
[9] A. Holm, Q. Stürzer, Y. Xu, and R. Weigel, "Investigation of surface acoustic waves on LiNbO3, quartz, and LiTaO3 by laser probing," *Microelectronic Engineering*, vol. 31, no. 1-4, pp. 123–127, Feb. 1996. [Online]. Available: https://linkinghub.elsevier.com/retrieve/pii/0167931795003347
[10] R. M. White and F. W. Voltmer, "Direct piezoelectric coupling to surface elastic waves," *Applied Physics Letters*, vol. 7, no. 12, pp. 314–316, Dec. 1965, publisher: American Institute of Physics. [Online]. Available: https://aip.scitation.org/doi/10.1063/1.1754276
[11] F. Voltmer, E. Ippen, R. White, T. Lim, and G. Farnell, "Measured and calculated surface-wave velocities," *Proceedings of the IEEE*, vol. 56, no. 9, pp. 1634–1635, 1968. [Online]. Available: http://ieeexplore.ieee.org/document/1448620/
[12] A. Holm, R. Weigel, P. Russer, and W. Ruile, "A laser probing system for characterization of SAW propagation on LiNbO/sub 3/, LiTaO/sub 3/, and quartz," in *1996 IEEE MTT-S International Microwave Symposium Digest*, vol. 3. San Francisco, CA, USA: IEEE, 1996, pp. 1541–1544. [Online]. Available: http://ieeexplore.ieee.org/document/512230/

V. Biography Section

If you have an EPS/PDF photo (graphicx package needed), extra braces are needed around the contents of the optional argument to biography to prevent the LaTeX parser from getting confused when it sees the complicated `\includegraphics` command within an optional argument. (You can create your own custom macro containing the `\includegraphics` command to make things simpler here.)

If you include a photo:

Michael Shell Use `\begin{IEEEbiography}` and then for the 1st argument use `\includegraphics` to declare and link the author photo. Use the author name as the 3rd argument followed by the biography text.

If you will not include a photo:

John Doe Use `\begin{IEEEbiographynophoto}` and the author name as the argument followed by the biography text.